Impacts of timing, length, and intensity of behavioral interventions to COVID-19 dynamics: North Carolina county-level examples

Claire Quiner[*], Kasey Jones, Georgiy Bobashev

RTI International, 3040 E. Cornwallis Road, PO Box 12194, Research Triangle Park, NC, 27709, USA

ABSTRACT

We sought to examine how the impact of revocable behavioral interventions, e.g., shelter-in-place, varies throughout an epidemic, as well as the role that the proportion of susceptible individuals had on an intervention's impact. We estimated the theoretical impacts of start day, length, and intensity of interventions on disease transmission and illustrated them on COVID-19 dynamics in Wake County, North Carolina, to inform how interventions can be most effective. We used a Susceptible, Exposed, Infectious, and Recovered (SEIR) model to estimate epidemic curves with modifications to the disease transmission parameter (β). We designed modifications to simulate events likely to increase transmission (e.g., long weekends, holiday seasons) or behavioral interventions likely to decrease it (e.g., shelter-in-place, masking). We compared the resultant curves' shape, timing, and cumulative case count to baseline and across other modified curves. Interventions led to changes in COVID-19 dynamics, including moving the peak's location, height, and width. The proportion susceptible, at the start day, strongly influenced their impact. Early interventions shifted the curve, while interventions near the peak modified shape and case count. For some scenarios, in which the transmission parameter was decreased, the final cumulative count increased over baseline. We showed that the timing of revocable interventions has a strong impact on their effect. The same intervention applied at different time points, corresponding to different proportions of susceptibility, resulted in qualitatively differential effects. Accurate estimation of the proportion susceptible is critical for understanding an intervention's impact.

The findings presented here provide evidence of the importance of estimating the proportion of the population that is susceptible when predicting the impact of behavioral infection control interventions. Greater emphasis should be placed on the estimation of this epidemic component in intervention design and decision-making.

Our results are generic and are applicable to other infectious disease epidemics, as well as to future waves of the current COVID-19 epidemic. Developed into a publicly available tool that allows users to modify the parameters to estimate impacts of different interventions, these models could aid in evaluating behavioral intervention options prior to their use and in predicting case increases from specific events.

© 2022 The Authors. Publishing services by Elsevier B.V. on behalf of KeAi Communications Co. Ltd. This is an open access article under the CC BY-NC-ND license (http://creativecommons.org/licenses/by-nc-nd/4.0/).

---

* Corresponding author.
  E-mail address: cquiner@rti.org (C. Quiner).

1. Introduction

The major public health crisis of the COVID-19 pandemic has led to more than 800,000 deaths in the United States (USA FACTS, 2022) and more than 5,000,000 deaths worldwide (Johns Hopkins University, 2022). International, federal, state, and local governments have responded with interventions (quarantine, mandates, travel restrictions, school, and business closings, etc.) designed to delay and attenuate the severity of the waves of the pandemic until medical countermeasures could be developed and employed. The psychological and economic impacts from prolonged interventions indicate that highly restrictive interventions should be reserved for when they are most effective (Brooks et al., 2020).

Past studies have shown that seasonality should be considered when designing interventions. Previously, we demonstrated that travel restrictions could lead to a delay in the peak of the epidemic curve, shifting it into a high transmissibility season (Institute for Health Metrics and Evaluation, 2021). An example of this is India, which imposed significantly restrictive COVID-19 behavioral interventions at the beginning of the pandemic, (Gupta et al., 2021; Lee et al., 2020). However, it entered the 2021 Holi holiday, which coincided with its crowd-forming, multistage state election season (Aljazeera, 2021) with <95% of its population susceptible, an estimate based on the reported cumulative case count (Worldometer, 2021). The convergence of high susceptibility with a drastic increase in contact rates led to a sizable surge in cases and deaths in India.

Mathematical models have been used to forecast epidemic dynamics that can be used to guide intervention decision-making (Alvarez et al., 2014; Azam et al., 2020; Kibachio et al., 2020). Predicting the impact of enforcing and lifting revocable behavioral interventions, e.g., school closings, shelter-in-place orders, and mask mandates used throughout the current SARS-CoV-2/COVID-19 pandemic, can lead to their optimal use. These interventions provide protection only for as long as they are enforced; once lifted, epidemic dynamics will change again, making the timing and length of an intervention an important predictor of its impact.

Two of the main drivers of epidemiological dynamics are the number of infectious and the proportion of susceptible individuals. While significant focus is placed on the estimate of infectious individuals for these models (Institute for Health Metrics and Evaluation, 2021; Kissler et al., 2020; Reiner et al., 2021; Ritchie et al., 2020; Russell et al., 2020), less effort is placed on estimating the susceptible population (Bobashev et al., 2000). In a pandemic of a novel pathogen, such as SARS-CoV-2, 100% of the population is considered susceptible at the start. As the pandemic progresses, the dynamics of susceptibility can be deduced from models, or more accurately, via serosurveys of a representative sample. The impact of ensuant emergent variants, each of which can have unique viral dynamics and interaction with preexisting immunity (Cosar et al., 2021; Kissler et al., 2021), can also be incorporated into estimates of the susceptible population and may allow for quicker and more accurate estimation of this parameter than others.

We used Susceptible, Exposed, Infectious, and Recovered (SEIR) models to assess the role of the susceptible population in predicting the ensuant epidemic dynamics resulting from an intervention; we also illustrated the differential effects of the same intervention, applied at different timepoints. We considered a theoretical epidemic curve for generic estimates, as well as an epidemic curve calculated using COVID-19 cases in Wake County, North Carolina, for a practical application. The results presented here emphasize the utility of estimating the susceptible population as a critical component in informed interventions.

Our study has important implications for predicting this optimal time and for the overall impact of applying and lifting interventions throughout an epidemic. Our results are generic and are applicable to other infectious disease epidemics and new waves of the current COVID-19 epidemic.

2. SEIR modeling

To illustrate the impact that behavioral interventions, designed to reduce contact rate, and periods of increased contact rate, e.g., holiday seasons, would have on COVID-19 cases, we considered a commonly used SEIR paradigm.

2.1. Model assumptions

For simplicity, we assumed heterogeneous mixing, equal infectiousness of all infected individuals, and equal susceptibility of all people. For these purposes, a susceptible individual is someone who has not yet been infected with SARS-CoV-2. These assumptions lead to a well-known mass-action principle that states that the incidence rate is based on the product of the proportions of infected and susceptible individuals SI with some proportionality coefficient β, which can be interpreted as a transmission rate. This coefficient singly summarizes contact rate between susceptible and infected individuals, social structure, and the probability of transmitting disease given the contact. Based on this assumption, disease dynamics could be represented by a well-known system of differential equations (Anderson & May 1991).

2.2. Theoretical SEIR model of COVID-19 epidemic curve

We used a commonly used SEIR paradigm. A population was divided into four dynamic subpopulations with S(t), E(t), I(t) and R(t) denoting the proportions of susceptible, exposed, infectious, and recovered populations, respectively. To represent the total population, these proportions must add to 1.

$$1 = S(t) + E(t) + I(t) + R(t)$$

Model-based estimation of the change in susceptible population requires the disease transmission parameter β.

$$\frac{dS(t)}{dt} = -\beta(t)S(t)I(t)$$

The proportionality coefficient β is a scaled number of contacts an individual makes per day and a probability of getting infected when there is contact between a susceptible and infectious person. This parameter is affected by policy and human behavior. Its value changes geographically and in time.

Those susceptible who got infected become exposed (infected but not yet infectious). Concurrently, a proportion of the exposed group will become infectious and move to the infectious population. The rate of progression for an individual from the exposed to the infectious state is α, where α is an inverse of the latency period (parameterized for COVID to be 5 days).

$$\frac{dE(t)}{dt} = \beta(t)S(t)I(t) - \alpha E(t)$$

Infectious individuals will recover from their infection at a rate of γ, the average recovery time for COVID-19 patients. They recover with permanent immunity, a simplifying assumption we currently make for illustration purposes.

$$\frac{dI(t)}{dt} = \alpha E(t) - \gamma I(t)$$

Every infectious individual eventually recovers and thus all infected individuals recover by the end of the outbreak. Again, deaths are ignored for the simplicity of presentation. Early in the COVID-19 pandemic, reinfection was thought to be rare, and therefore we did not add a pathway for recovered individuals to return to the susceptible population.

$$\frac{dR(t)}{dt} = \gamma I(t)$$

2.2.1. Modeling behavior interventions by modifying the disease transmission parameter, β, in the theoretical model

Behavioral interventions, including social distancing; mask wearing; sheltering-in-place; and school, office, and business closings theoretically reduce the probability of viral transmission by reducing or eliminating contact between susceptible and infectious individuals, which in turn reduces the value of β. We designed a series of modifications to β to simulate decreases in transmission due to interventions by decreasing β by either 33% or 75% (to account for varying efficacy of interventions) for 60, 90, or 120 consecutive days. Conversely, single-day events (e.g., concerts or sporting matches) or holiday periods (e.g., Thanksgiving weekend) can increase contact rates. We designed modifications to β that would simulate the estimated increase in transmission from daylong events, long weekends, or longer holiday periods by doubling the value of β, for 1, 5, or 10 consecutive days.
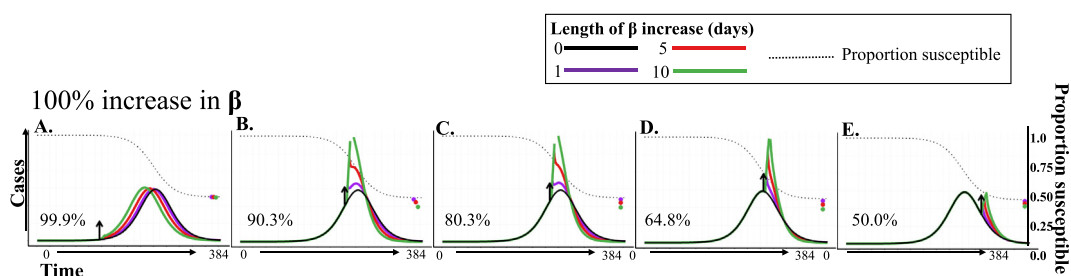
Fig. 1A. E: Predicted epidemic curve of COVID-19 cases resulting from an increase in β (β x 2), at different time points in the epidemic curve (black arrow), for different lengths of time: No increase = black, increase for 1 day = purple, 5 days = red, and 10 days = green. The final proportion susceptible for each β increase scenario is indicated by a dot at time = 1000, whose color corresponds to its β increase length. The percentage susceptible at the time of the modification is listed at the bottom left corner. It is plotted using a dotted black line throughout the time course.

We applied the increased and decreased β parameter modifications described above to the model at five different timepoints, each of which corresponded to a distinct case count and proportion of susceptibility. To illustrate the modifications' effects, SEIR models with and without modifications to β were run for a period of 600 days (T = 600) (Fig. 1), which was sufficient time to see the rise and fall of the baseline peak (no modification to β). We also considered T = 1000 (Figs. 2 and 3), which was sufficient to observe the peaks delayed by decreasing β. We plotted the epidemic curves resulting from these modifications and visually compared each peak's height, width, and timing to baseline and across other modified models. The start day of the modification is indicated on each graph by an arrow; whether β was increased or decreased is indicated by the arrow's direction. To estimate the modification's impact on cumulative cases, we also plotted the proportion susceptible as a single point on the graph.

To differentiate the role of case count from that of proportion susceptible in predicting a modification's impact, we made identical modifications on parallel but opposite sides of an epidemic curve (pre- and post-peak), when the case counts were the same but the proportion susceptible was different.

2.3. Wake County, North Carolina, SEIR model of COVID-19 epidemic curve

A theoretical model is an idealization that ignores human response and adaptive behavior and produces a single-peak characteristic trajectory. However, actual disease dynamics can include multiple waves/peaks associated with population heterogeneity, seasonality, and adaptive human response.

2.3.1. Model parameters

We parameterized SEIR models to represent COVID-19 infectious dynamics in Wake County, North Carolina. The selection of this population was guided by the community size (about one million residents) and urbanicity (98% urban), partially justifying the assumption of homogeneous mixing.

We used biological parameters of infectivity rate α (Wiersinga et al., 2020) and recovery rate γ (Wölfel et al., 2020)and estimated the dynamically changing transmission parameter β. The transmission parameter was estimated from the effective reproductive rate, which was derived from the growth rate of infective individuals. Reported case counts were obtained from publicly available data sources (USA FACTS, 2021).

To estimate daily β values for Wake County, we first estimated the true number of infections (TI) per day in Wake County. We assumed that reported cases, $RC(t)$, were linked to daily infections through the *case multipliers, $X(t)$* , such that: $TI(t) = RC(t)*X(t)$. These multipliers could be estimated by surveying the general population and estimating the number of recovered individuals (e.g., individuals with SARS-CoV2 antibodies). These estimates provide the scaling factor for the cumulative number of infected individuals, linking it to the cumulative number of reported cases. As this information was limited, we parameterized these values by reviewing published literature on the level of underreporting of COVID-19 infections (Indiana University, 2020; Li et al., 2020; Menachemi et al., 2020; Rosenberg et al., 2020). A multiplier of 10 was used for the first 90 days, after which a linearly decreasing multiplier from 10 to 4 was used through 270, and a multiplier of 4 thereafter.

$$X = 10, 0 < t < 90 \quad X = 10 - \frac{(10-4)}{180}*(t-90), 90 < t < 270 \quad X = 4, t > 270$$
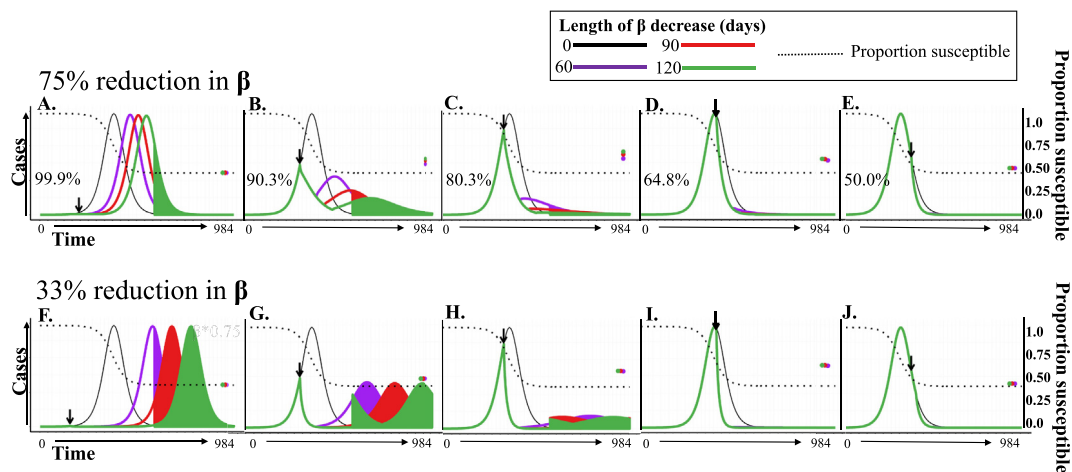
Fig. 2A. J: Predicted epidemic curve of COVID-19 cases resulting from a decrease in β, which reduces transmission by 75% (A–E) or 33% (F–J), at different time points in epidemic curve (black arrow), for different lengths of time: No decrease = black, decrease for 60 days = purple, 90 days = red, and 120 days = green.
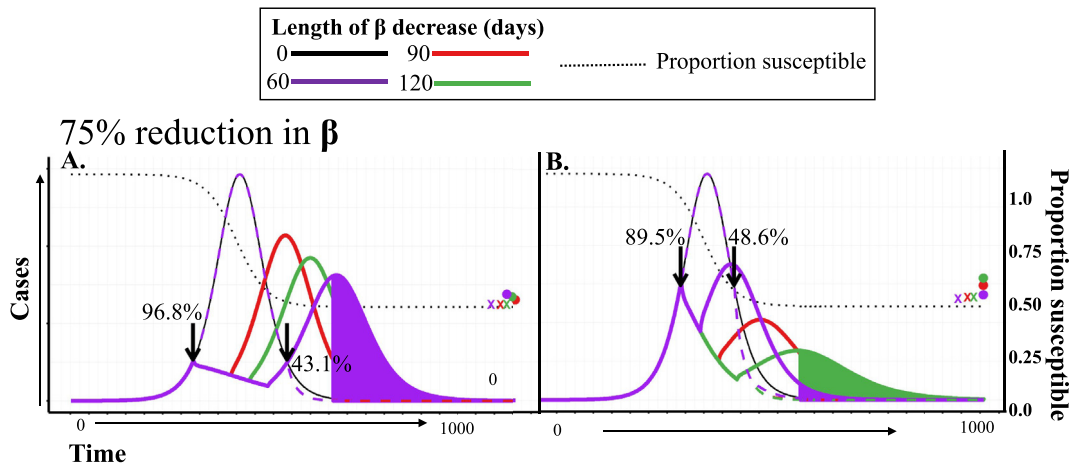
Fig. 3A. B: Predicted epidemic curve of COVID-19 cases resulting from a decrease in β at different time points in theoretical epidemic curve (black arrows), when there are similar case counts and different proportions susceptible. A. β decrease applied, for varying lengths of time, when either 96.8% (solid lines) or 43.1% (dotted lines) of the population is susceptible. B. β decrease applied when either 89.5% (solid line) or 48.6% (dotted line) of the population is susceptible. The final proportion susceptible for each β decrease scenario is indicated by a dot (decrease on left hand side of curve) or an "X" (decrease on right hand side of curve) at time = 1000, whose color corresponds to its β decrease length.

The estimated case infections were then smoothed using a cubic spline function to reduce issues with underreporting on weekends and holidays (where zero new infections were routinely reported).

Using the smoothed reported infection cases, we estimated β by (1) calculating the growth rate in new infections, (2) converting this to an estimate of the reproductive number, and (3) estimating β by reversing the βSI equation (Stoner et al., 2021). Growth rate was calculated using the following formula:

$$GR(t) = \frac{TI(t)}{TI(t-x)}^{\frac{1}{x}} - 1$$

We chose x = 7 to represent weekly changes in the growth rate and a change in infections between weeks. We assumed the reporting of cases would be inconsistent over the course of a week (e.g., less reporting on Sundays than on Mondays), but reporting across weeks would be fairly consistent. Next, we calculated the reproductive number R, which reflects how many individuals an infectious person infects during the infectious period (Wallinga & Lipsitch, 2007).

$$R(t) = \left(1 + \frac{GR(t)}{\alpha}\right) * \left(1 + \frac{GR(t)}{\gamma}\right) \quad R(t) = \left(1 + GR\left(t\right) * 5\right) * \left(1 + GR\left(t\right) * 6\right)$$

After the reproductive number was estimated, an estimate for β was calculated by rearranging the βSI equation. Let *CI(t)* represent the cumulative number of infections at time *t*, and *P* represent the population of Wake County. This allows estimation of *S(t)* due to the assumption that no recovered individuals will become susceptible again.

$$\beta(t) = \frac{R(t) * \gamma}{1 - \frac{CI(t)}{P}}$$

This set of equations produced a β estimate for each day where data was available and were used in an SEIR model to generate the Wake County, North Carolina, COVID-19 epidemic curves used in these analyses. Projections for β were not made beyond available data. The calculated value of β for the last day of available data was used to run the SEIR model to create infection projections. The projected infections were divided by the case multipliers described above to estimate the number of reported cases.

2.3.2. Modeling behavior interventions by modifying the disease transmission parameter, β, in the Wake County model

We applied the same modifications to the transmission parameter β as those used on the theoretical model (described above) to five different time points on this curve and plotted results similarly.

3. Results

3.1. Theoretical COVID-19 epidemic curve

We observed three different categories of impacts to the epidemic curve, resulting from modifications to β: (1) shifting the curve to the left (increase in β) or to the right (decrease in β) without an observable change in cumulative case count; (2) increasing or decreasing peak height; or (3) flattening the curve to zero.

When we applied modifications to β (increases and decreases) early in the curve—when the case count was low and the proportion of the population susceptible was high—the curve was shifted without an observable change in the cumulative case count or in the height of the peak. However, the peak was moved to different points in time (Figs. 1A, 2A and 2J).

When we applied modifications to β (increases and decreases) when the case count was higher despite a lower proportion of susceptibility (90.3%), both modifications shifted the curve and caused an observable change in peak height that was proportional to the length and intensity of the modification (Figs. 1B, 2B and 2G). The final proportion susceptible in these models was different from baseline, indicating that these modifications to β modified the cumulative case count and shifted the timing of the curve when applied later in an epidemic, compared with early interventions, which only shifted the curve.

For modifications where β was increased, this pattern of increasing both the cumulative case count and the height of the peak continued (Fig. 1C and D) until the proportion susceptible reached 50% (Fig. 1E), at which point the β modification had minimal impact. Conversely, where β was decreased, a flattening of the curve could be observed when 80% of the population was susceptible and transmission was reduced by 33% (Fig. 2C), or when only 90% was susceptible and transmission was reduced by 75% (Fig. 2G). At both levels of transmission reduction, this pattern continued more drastically as the proportion susceptible decreased, even as number of cases increased (Fig. 2C–D and H–I).

Increases in β when the proportion susceptible was 50% resulted in a short and narrow peak of cases before returning to baseline numbers (Fig. 1E). In decreasing the β at 50% susceptibility, the number of cases dropped to nearly zero however, the decrease in the cumulative number infected was minimal as compared to baseline (Fig. 2E and J).

The modifications to β with the largest impact on cumulative case count and peak height were those applied near the peak when the proportion susceptible was above 50%. By contrast, early modifications to β changed the timing of the peak while maintaining the shape of the curve and cumulative cases.

To differentiate the effects that the number of cases and the proportion susceptible have on predicting the impact of infection control policies, we modeled β decreases at two parallel points of the theoretical curve and observed that the contribution of proportion susceptible to the impact of the modification differed with its timing of application (Fig. 3A and B). When the modifications were applied when number of cases were low, both had an equal, minimal impact on the cumulative case counts; however, the early intervention shifted, shortened, and widened the curve, while the late intervention flattened it (Fig. 3A). In contrast, when the same modifications were applied closer to the peak (Fig. 3B), both decreased cumulative case counts more than the same intervention did when case counts were low (Fig. 3A). The early intervention was more impactful than the later one.

3.2. COVID-19 epidemic curve of Wake County, North Carolina

To better understand how timing and intensity of interventions affects an actual epidemic curve, we decreased the estimated β on the epidemic curve of reported COVID-19 cases in Wake County, North Carolina, using identical lengths and intensities as the modifications to β in the theoretical model (Fig. 2). We also used similar proportions of population susceptibility. In addition to the three patterns observed on the theoretical model, a fourth pattern was observed in this case: a resurgence, or new peak, of cases at later months.

A β modification of a 33% reduction in transmission applied prior to October 2020 resulted in more cumulative cases at the end of the time series (Fig. 4A–C), as did β decreases of 75% reduction in transmission prior to July 2020 (Fig. 4F and G). Applied when there was a high proportion susceptible and minimal cases, these decreases shortened the 2020/21 holiday season peak, however, there was a resurgence in the months that followed, with peaks higher than those in the actual curve.

The decrease of β was applied on December 1, 2020, in between two significant holiday/travel periods in the United States (Fig. 4D). All β decreases made on this date drastically reduced the height of the peak. Subsequently, there were fewer cumulative cases. In the models where cases did resurge, the height of the peak was much lower than in the actual curve.

A 120-day, 75% reduction in transmission during a plateau when 88.1% were susceptible was sufficient to flatten the curve and reduce the cumulative number of cases; a 60-day reduction at that point allowed for a later resurgence, which peaked during winter months and increased the cumulative cases (Fig. 4H).

To differentiate the effects that the number of cases and the proportion susceptible has on predicting the impact of infection control policies, we modeled β decreases at two different parallel points of the Wake County curve and observed that their contributions differed with the timing of the application of the β decrease (Fig. 5A and B). Decreasing β when there were minimal cases (~100) and either 97.1% or 88.8% proportion susceptible increased the cumulative number of cases over baseline. Although all modifications reduced the peak height and width during the holiday season, each resulted in a later resurgence with peaks in the summer and fall months, (when applied at 97.1% susceptibility) or during the fall and winter months, (when applied at 97.1% susceptibility) (Fig. 5A). Using the same approach, at a higher case count (~300), β was decreased when the proportion susceptible was lower—84.1% or 66.9%—the decrease at 84.1% susceptible resulted in more
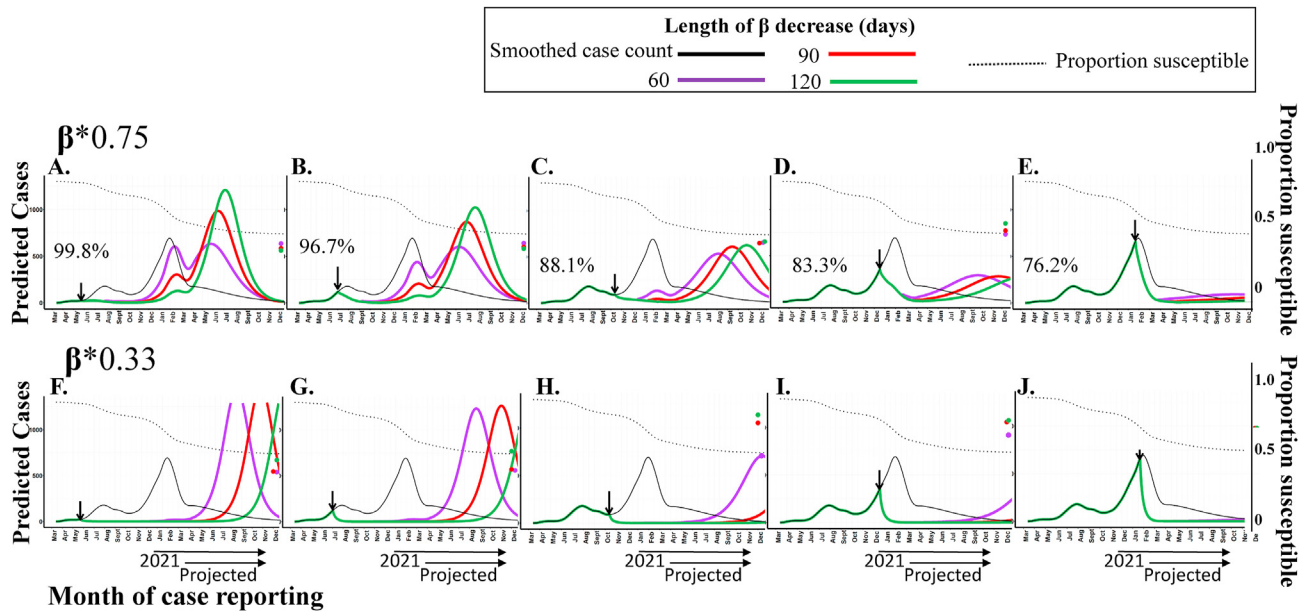
Fig. 4A. E: Predicted epidemic curve of COVID-19 cases resulting from a decrease in β, which reduces transmission by 75% (A–E) or 33% (F–J) at different time points in epidemic curve (black arrow) for different lengths of time: Actual curve = black, decrease for 30 days = purple, 60 days = red, and 90 days = green.
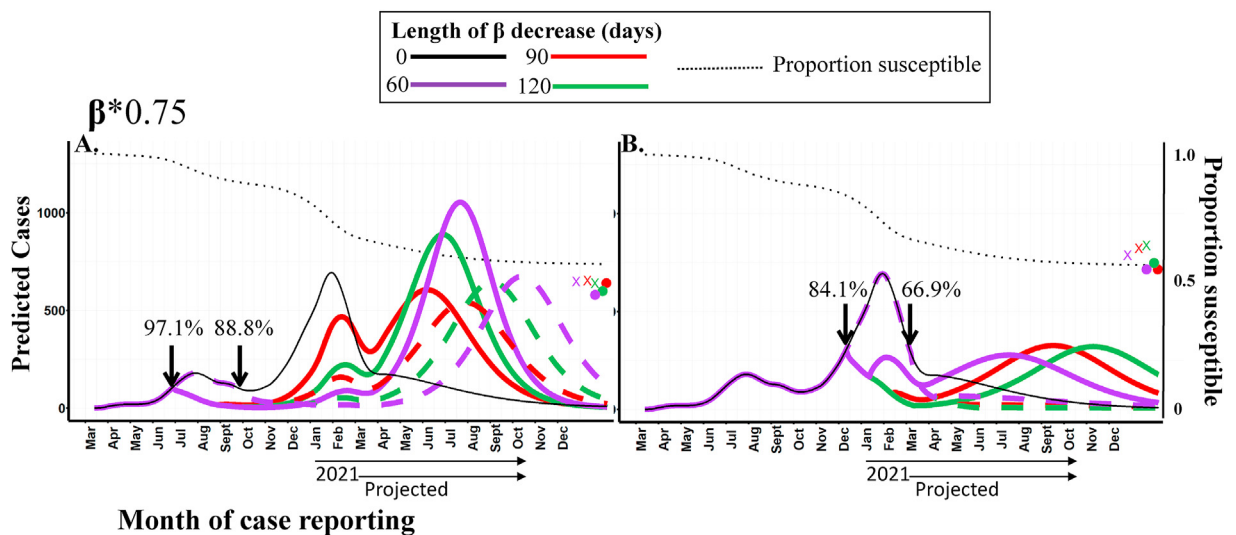
Fig. 5A. B: Predicted epidemic curve of COVID-19 cases resulting from a decrease in β, at different time points in theoretical epidemic curve (black arrows), when there are similar case counts but different proportions susceptible. A. β decreases applied when there are 100 cases and either 97.1% (solid line) or 88.8% (dotted line) of the population is susceptible, B. β decreases applied when there are 300 cases and either 84.1% (solid line) or 66.9% (dotted line) of the population is susceptible. The final proportion susceptible, for each β decrease scenario, is indicated by a dot (decrease on left hand side of curve) or an "X" (decrease on right hand side of curve), whose color corresponds to its β decrease length.

cumulative cases, attributed to a resurgence, whereas the decrease (66.9% susceptible) flattened the curves and maintained or reduced the cumulative case count, as compared to baseline (Fig. 5B).

Correspondingly, an increase in the transmission values early in the pandemic to pre-pandemic levels (lifting all restrictions) would result in a much larger increase in incidence than it would towards the end of the epidemic.

4. Discussion

We used SEIR models to illustrate differential effects of the same intervention, modified by the susceptible population at time of its application. We illustrated that when the proportion susceptible is high, increasing the transmission parameter (analogous to lifting interventions) would result in a larger increase in cases as compared to doing so when >50% of the population is in the recovered state, when the impact would be minimal.

While this work shows the value in estimating the proportion susceptible, accurate estimates of this proportion face many challenges. This model assumes permanent immunity from SARS-CoV-2 infection; however, reinfection has been documented (Chen et al., 2020; Nainu et al., 2020). Vaccine and booster availability and rollout (Oliver et al., 2020, 2021) have increased the proportion of individuals in the recovered state, an unknown proportion of which had some prior immunity from infection. Emergent variants and waning immunity make an unknown proportion of those who were in the recovered state both susceptible and potentially infectious once again. The severity of current and future waves depends on vaccine efficacy and waning immunity in the face of numerous and continuously emergent variants. Longitudinal, population-based seroprevalence studies (Stringhini et al., 2020) and estimates of the transmission parameter, reporting rate, and proportion susceptible are all needed to accurately recalibrate these models. Nonetheless, the key results presented here, related to the importance of the timing and intensity of behavioral interventions, are valid for a broad range of epidemics.

We developed a Shiny tool, described in detail in Supplemental Figures (SF) 1 and 2, to allow for assessment of theoretical interventions. The tool allows the user to incorporate parameter information as estimates become available and are relevant to the region. By defining the desired outcome, e.g., to reduce cumulative number of cases, to delay an epidemic peak, or to reduce the peak during a holiday season, users can identify the optimal timing, length, and intensity of policies estimated as necessary to reach that goal.

We did not consider the translation of actual intervention effects into specific changes in transmission. These estimates are beyond the scope of this study and would vary with each locality with the impacts of population density, adherence, and other locale-specific factors.

5. Conclusions

Simulation modeling of revocable, behavioral interventions demonstrate that the proportion of the population susceptible predicts the intervention's impact. Our study can inform predicting the overall impact and the optimal timing for applying and lifting interventions throughout an epidemic.

Dependent on the timing, intensity, and length, interventions can (1) shift the epidemic curve without impacting cumulative case count; (2) change peak height; (3) flatten the curve, or (4) create a new curve at a later point in time. The susceptible proportion at the time of application predicts an intervention's impact; more emphasis should be placed on estimating this epidemic component when planning for and recommending interventions. These results are generic and are applicable to other infectious disease epidemics and new waves of the current COVID-19 epidemic.

Funding

Author contributions

Claire Quiner: Software; Formal analysis; Investigation, Writing - Original Draft, Visualization; Kasey Jones: Methodology, Validation; Investigation; Data Curation; Resources, Writing - Review & Editing. Georgiy Bobashev: Project administration, Conceptualization, Writing - Review & Editing, Supervision, Project administration, Funding acquisition.

Declaration of competing interest

All authors declare no conflict of interest.

Acknowledgements

Appendix A. Supplementary data

Supplementary data to this article can be found online at https://doi.org/10.1016/j.idm.2022.08.002.

References

Aljazeera. (2021). India celebrates Holi amid alarming surge in COVID cases, 3/29/2021 *Aljazeera* https://www.aljazeera.com/gallery/2021/3/29/in-pictures-indians-celebrate-holi-as-virus-cases-surge.

Alvarez, J., Bezos, J., de la Cruz, M. L., Casal, C., Romero, B., Domínguez, L., de Juan, L., & Pérez, A. (2014). Bovine tuberculosis: Within-herd transmission models to support and direct the decision-making process. *Research in Veterinary Science, 97*(Suppl), S61–S68. https://doi.org/10.1016/j.rvsc.2014.04.009

Anderson, R. M., & May, R. M. (1991). *Infectious diseases of humans: Dynamics and control, 1991.* Cambridge University Press.

Azam, J. M., Are, E. B., Pang, X., Ferrari, M. J., & Pulliam, J. R. C. (2020). Outbreak response intervention models of vaccine-preventable diseases in humans and foot-and-mouth disease in livestock: A protocol for a systematic review. *BMJ Open, 10*(10), Article e036172. https://doi.org/10.1136/bmjopen-2019-036172

Bobashev, G. V., Ellner, S. P., Nychka, D. W., & Grenfell, B. T. (2000). Reconstructing susceptible and recruitment dynamics from measles epidemic data. *Mathematical Population Studies, 8*(1), 1–29. https://doi.org/10.1080/08898480009525471

Brooks, S. K., Webster, R. K., Smith, L. E., Woodland, L., Wessely, S., Greenberg, N., & Rubin, G. J. (2020). The psychological impact of quarantine and how to reduce it: Rapid review of the evidence. *Lancet (London, England), 395*(10227), 912–920. https://doi.org/10.1016/S0140-6736(20)30460-8

Chen, D., Xu, W., Lei, Z., Huang, Z., Liu, J., Gao, Z., & Peng, L. (2020). Recurrence of positive SARS-CoV-2 RNA in COVID-19: A case report. *International Journal of Infectious Diseases : IJID : official publication of the International Society for Infectious Diseases, 93*, 297–299. https://doi.org/10.1016/j.ijid.2020.03.003

Cosar, B., Karagulleoglu, Z. Y., Unal, S., Ince, A. T., Uncuoglu, D. B., Tuncer, G., Kilinc, B. R., Ozkan, Y. E., Ozkoc, H. C., Demir, I. N., Eker, A., Karagoz, F., Simsek, S. Y., Yasar, B., Pala, M., Demir, A., Atak, I. N., Mendi, A. H., Bengi, V. U., et al., … (2021). *SARS-CoV-2 Mutations and their viral variants.* Cytokine & growth factor reviews, Article S1359. https://doi.org/10.1016/j.cytogfr.2021.06.001, 6101(1321)00053-00058.

Gupta, M., Mohanta, S. S., Rao, A., Parameswaran, G. G., Agarwal, M., Arora, M., Mazumder, A., Lohiya, A., Behera, P., Bansal, A., Kumar, R., Meena, V. P., Tiwari, P., Mohan, A., & Bhatnagar, S. (2021). Transmission dynamics of the COVID-19 epidemic in India and modeling optimal lockdown exit strategies. *International Journal of Infectious Diseases : IJID : official publication of the International Society for Infectious Diseases, 103*, 579–589. https://doi.org/10.1016/j.ijid.2020.11.206

Hopkins University, J. (2022). *fFig2022, 1/13.* Johns Hopkins Coronavirus Resource Center.

Indiana University. (2020). *IU, ISDH release preliminary findings about impact of COVID-19 in Indiana, 05/13/2020.*

Institute for Health Metrics and Evaluation. (2021). IHME COVID-19 Projections (translator, Trans.). In *Book IHME COVID-19 Projections.*

Kibachio, J., Mwenda, V., Ombiro, O., Kamano, J. H., Perez-Guzman, P. N., Mutai, K. K., Guessous, I., Beran, D., Kasaie, P., Weir, B., Beecroft, B., Kilonzo, N., Kupfer, L., & Smit, M. (2020). Recommendations for the use of mathematical modelling to support decision-making on integration of non-communicable diseases into HIV care. *Journal of the International AIDS Society, 23*(Suppl 1), Article e25505. https://doi.org/10.1002/jia2.25505. Suppl 1.

Kissler, S. M., Fauver, J. R., Mack, C., Tai, C. G., Breban, M. I., Watkins, A. E., Samant, R. M., Anderson, D. J., Metti, J., Khullar, G., Baits, R., MacKay, M., Salgado, D., Baker, T., Dudley, J. T., Mason, C. E., Ho, D. D., Grubaugh, N. D., & Grad, Y. H. (2021). Viral dynamics of SARS-CoV-2 variants in Vaccinated and Unvaccinated persons. *New England Journal of Medicine, 385*(26), 2489–2491. https://doi.org/10.1056/NEJMc2102507

Kissler, S. M., Tedijanto, C., Goldstein, E., Grad, Y. H., & Lipsitch, M. (2020). Projecting the transmission dynamics of SARS-CoV-2 through the postpandemic period. *Science (New York, N.Y.), 368*(6493), 860–868. https://doi.org/10.1126/science.abb5793

Lee, K., Sahai, H., Baylis, P., & Greenstone, M. (2020). *Job loss and behavioral change: The unprecedented effects of the India lockdown in Delhi.* University of Chicago, Becker Friedman Institute for economics working paper, 2020-65.

Li, R., Pei, S., Chen, B., Song, Y., Zhang, T., Yang, W., & Shaman, J. (2020). Substantial undocumented infection facilitates the rapid dissemination of novel coronavirus (SARS-CoV-2). *Science, 368*(6490), 489. https://doi.org/10.1126/science.abb3221

Menachemi, N., Yiannoutsos, C. T., Dixon, B. E., Duszynski, T. J., Fadel, W. F., Wools-Kaloustian, K. K., Needleman, N. U., Box, K., Caine, V., Norwood, C., Weaver, L., & Halverson, P. K. (2020). Population point Prevalence of SARS-CoV-2 infection based on a Statewide random Sample — Indiana, April

25–29, 2020 (translator, Trans.). In *Book population point Prevalence of SARS-CoV-2 infection Based on a Statewide random Sample — Indiana, April 25–29, 2020. CDC Morbidity and Mortality weekly Report (MMWR)*.

Nainu, F., Abidin, R. S., Bahar, M. A., Frediansyah, A., Emran, T. B., Rabaan, A. A., Dhama, K., & Harapan, H. (2020). SARS-CoV-2 reinfection and implications for vaccine development. *Human Vaccines & Immunotherapeutics, 16*(12), 3061–3073. https://doi.org/10.1080/21645515.2020.1830683

Oliver, S. E., Gargano, J. W., Marin, M., Wallace, M., Curran, K. G., Chamberland, M., McClung, N., Campos-Outcalt, D., Morgan, R. L., Mbaeyi, S., Romero, J. R., Talbot, H. K., Lee, G. M., Bell, B. P., & Dooling, K. (2020). The Advisory Committee on Immunization Practices' Interim Recommendation for Use of Pfizer-BioNTech COVID-19 vaccine - United States, December 2020. *MMWR. Morbidity and mortality weekly report, 69*(50), 1922–1924. https://doi.org/10.15585/mmwr.mm6950e2

Oliver, S. E., Gargano, J. W., Marin, M., Wallace, M., Curran, K. G., Chamberland, M., McClung, N., Campos-Outcalt, D., Morgan, R. L., Mbaeyi, S., Romero, J. R., Talbot, H. K., Lee, G. M., Bell, B. P., & Dooling, K. (2021). The Advisory Committee on Immunization Practices' Interim Recommendation for Use of Moderna COVID-19 vaccine - United States, December 2020. *MMWR. Morbidity and mortality weekly report, 69*(5152), 1653–1656. https://doi.org/10.15585/mmwr.mm695152e1

Reiner, R. C., Barber, R. M., Collins, J. K., Zheng, P., Adolph, C., Albright, J., Antony, C. M., Aravkin, A. Y., Bachmeier, S. D., Bang-Jensen, B., Bannick, M. S., Bloom, S., Carter, A., Castro, E., Causey, K., Chakrabarti, S., Charlson, F. J., Cogen, R. M., Combs, E., et al., … (2021). Modeling COVID-19 scenarios for the United States. *Nature Medicine, 27*(1), 94–105. https://doi.org/10.1038/s41591-020-1132-9

Ritchie, H., Mathieu, E., Rodés-Guirao, L., Appel, C., Giattino, C., Ortiz-Ospina, E., Hasell, J., Macdonald, B., Beltekian, D., & Roser, M. (2020). Coronavirus pandemic (COVID-19) (translator, Trans.). In *Book coronavirus pandemic (COVID-19) . OurWorldInData.org*.

Rosenberg, E. S., Tesoriero, J. M., Rosenthal, E. M., Chung, R., Barranco, M. A., Styer, L. M., Parker, M. M., Leung, S.-Y. J., Morne, J. E., Greene, D., Holtgrave, D. R., Hoefer, D., Kumar, J., Udo, T., Hutton, B., & Zucker, H. A. (2020). *Cumulative incidence and diagnosis of SARS-CoV-2 infection in*. New York: medRxiv. https://doi.org/10.1101/2020.05.25.20113050, 2020.2005.2025.20113050.

Russell, T. W., Golding, N., Hellewell, J., Abbott, S., Wright, L., Pearson, C. A. B., van Zandvoort, K., Jarvis, C. I., Gibbs, H., Liu, Y., Eggo, R. M., Edmunds, W. J., & Kucharski, A. J. (2020). Reconstructing the early global dynamics of under-ascertained COVID-19 cases and infections. *BMC Medicine, 18*(1), 332. https://doi.org/10.1186/s12916-020-01790-9

Stoner, M., Preiss, A., Endres-Dighe, S., Jones, K., Hadley, E., & Rhea, S. (2021). *Estimating the effective reproduction number of COVID-19 in North Carolina. Outbreak*.

Stringhini, S., Wisniak, A., Piumatti, G., Azman, A. S., Lauer, S. A., Baysson, H., De Ridder, D., Petrovic, D., Schrempft, S., Marcus, K., Yerly, S., Arm Vernez, I., Keiser, O., Hurst, S., Posfay-Barbe, K. M., Trono, D., Pittet, D., Gétaz, L., Chappuis, F., et al., … (2020). Seroprevalence of anti-SARS-CoV-2 IgG antibodies in Geneva, Switzerland (SEROCoV-POP): A population-based study. *Lancet (London, England), 396*(10247), 313–319. https://doi.org/10.1016/S0140-6736(20)31304-0

USA FACTS. (2021). North Carolina coronavirus cases and deaths (Translator, Trans.). In *Book North Carolina coronavirus cases and deaths*. USA FACTS.

USA FACTS. (2022). US coronavirus vaccine tracker (translator, Trans.). In *Book US Coronavirus vaccine tracker*. USA FACTS.

Wallinga, J., & Lipsitch, M. (2007). How generation intervals shape the relationship between growth rates and reproductive numbers. *Proceedings. Biological sciences, 274*(1609), 599–604. https://doi.org/10.1098/rspb.2006.3754

Wiersinga, W. J., Rhodes, A., Cheng, A. C., Peacock, S. J., & Prescott, H. C. (2020). Pathophysiology, transmission, Diagnosis, and Treatment of coronavirus disease 2019 (COVID-19): A review. *JAMA, 324*(8), 782–793. https://doi.org/10.1001/jama.2020.12839

Wölfel, R., Corman, V. M., Guggemos, W., Seilmaier, M., Zange, S., Müller, M. A., Niemeyer, D., Jones, T. C., Vollmar, P., Rothe, C., Hoelscher, M., Bleicker, T., Brünink, S., Schneider, J., Ehmann, R., Zwirglmaier, K., Drosten, C., & Wendtner, C. (2020). Virological assessment of hospitalized patients with COVID-2019. *Nature, 581*(7809), 465–469. https://doi.org/10.1038/s41586-020-2196-x

Worldometer. (2021). *Coronavirus cases*, 8/31/2021. India.